

Design of starting a three phase induction motor using direct on-line, variable frequency drive, soft starting, and auto transformer methods

Yulianta Siregar¹, Yosephine Rotua Oktaviana Siahaan¹, Nur Nabila Binti Mohamed²,
Dedet Candra Riawan³, Muldi Yuhendri⁴

¹Department of Electrical Engineering, Universitas Sumatera Utara, Medan, Indonesia

²College of Engineering, University Technology MARA, Shah Alam, Malaysia

³Department of Electrical Engineering, Institut Teknologi Sepuluh Nopember, Surabaya, Indonesia

⁴Department of Electrical Engineering, Universitas Negeri Padang, Padang, Indonesia

Article Info

Article history:

Received Apr 27, 2024

Revised Sep 12, 2024

Accepted Sep 29, 2024

Keywords:

Auto transformer

Direct on-line

Soft starting

Three phase induction motor

Variable frequency drive

ABSTRACT

The problem with 3-phase induction motors is that when starting the motor, the motor starting current can reach five to seven times the nominal current. This research compares slip, starting current, bus voltage, acceleration torque, motor torque, energy savings, and kVAR from the direct on-line (DOL), variable frequency drive (VFD), soft starting, and autotransformer starting methods in the electrical transient analyzer program (ETAP) software. This research result shows that the fastest VFD slip reaches a steady state, namely at 11+ seconds. The lowest starting/starting current is owned by the VFD method, namely <20% full load amps (FLA) in the first 2 seconds. The lowest decrease in bus voltage at steady state was experienced by the VFD method, namely 0.8152%. The quickest acceleration torque reaches a steady state in the VFD method, namely in 11+ seconds. The soft starting method owns the lowest starting torque, namely 20.75%. The soft starting method has the largest energy savings, namely 148.02 kW. Of the several variables observed, the best starting method is the VFD method.

This is an open access article under the [CC BY-SA](https://creativecommons.org/licenses/by-sa/4.0/) license.



Corresponding Author:

Yulianta Siregar

Department of Electrical Engineering, Universitas Sumatera Utara

North Sumatera Province, Medan, Indonesia

Email: julianta_srg@usu.ac.id

1. INTRODUCTION

In the 3-phase induction motor industry, it is the type of motor that is most widely used, for example, in wood processing, textiles, and other industries. This type of motor is preferred because of its simple shape, reliable construction, easy operation and maintenance. In general, many industries use motors with varying capacities from small to large according to load requirements. This motor installation can be done individually or in groups. However, in its use, there is an initial problem, namely the continuous surge in starting current received by the winding or rotor on a three-phase induction motor that will damage the motor winding over a long period. When an induction motor is started and connected to a power system, the starter motor provides a low-impedance path to the system, thereby allowing a relatively high current from the power system to flow into the low-impedance path. This causes a sharp decrease in supply current to other nearby loads, which decreases voltage in the system [1].

The large starting current can cause a voltage drop and disrupt the operation of other equipment on the same network. Large currents can also produce excessive heat, which can damage the coil insulation and

shorten the machine's life [2], [3]. Induction motors produce inductive loads, which can reduce the power quality of the power system. This inductive load affects the power factor and power quality. The greater the inductive load, the worse the power factor or quality. The power factor will affect the economy. Therefore, additional reactive power is needed to overcome the induction load generated by the induction motor. This reactive power can be obtained from capacitor banks. There are several methods for starting induction motors, namely direct on-line (DOL) [4], [5], star delta (Y- Δ) [4]–[7], variable frequency drive (VFD) [8]–[11], soft starting [11]–[13], and auto-transformer [14], [15]. Meanwhile, ETAP (electrical transient analyzer program) is the most comprehensive solution for simulation, design, and analysis of generation, transmission, distribution, and industrial power systems [16], [17].

Generally, two important things must be considered when starting a 3-phase induction motor: the starting current taken from the supply line and the starting torque. The objectives of the study is the starting current must be kept small to avoid overheating the induction motor and excessive voltage drops in the network system. The starting torque should be about 50% to 100% higher than the expected load torque to ensure that the motor runs fairly quickly [18], [19].

This section includes several example studies and explains the work done to start directly online [5], [16], [18], [20]. The previous research regarding induction motor starting and start aided devices [17] compares starting current, reduced bus voltage drop, starting torque, and energy savings from each starting method of induction motor. The induction motor starting methods used in this research are VFD, capacitor starting, star delta, and auto-transformer. In this research, the best method for reducing the starting current is VFD, and the best method for saving energy is auto-transformer.

Research was also conducted by [5]; this compared VL-N, VL-L, total harmonic distortion (THD) VL-N, THD VL-L, THD I, and the starting current of each induction motor starting method. The induction motor starting methods used in this research are DOL, star delta, and VSD Altivar61. The results of this research, namely the acquisition of starting current from the third method, show that the Altivar61 VSD method produces the smallest starting current, and the rotational acceleration of the 3-phase motor becomes smoother.

Previous research by [18] also observed starting current, voltage drop, energy used, and investment costs from the DOL, star delta, auto-transformer, and soft starter starting methods. The results of this research are that from the four starting methods, it was found that the smallest starting current was obtained from the star delta method, the smallest used energy was obtained from the star delta method, the smallest voltage drop was obtained from the soft starter, the cheapest investment costs were obtained from the DOL method and the most expensive investment costs with the Soft Starter method.

The other previous research by [16] compared the starting current and starting torque from the auto transformer and VFD methods. The results of this research are simulations showing that the VFD method is better than the auto-transformer method. Furthermore, research by [20], this work addresses a novel method for minimizing the inrush of beginning current in polyphase induction motors by starting them without the need for primary voltage compensators. The crank driving mechanism of the motor rotates its rotor at a reasonable speed in the designated direction. The motor is then given its rated voltage. This is explained with the help of a case study on a 3-phase, 5-hp NGEF make motor, oscillographic recordings from the experiments, and comparisons with other starting methods.

Based on the problems explained and previous research background, this research provides a solution using a simulation and analysis comparing the DOL, VFD, soft starting, and auto transformer starting methods. The parameters compared from the four starting methods are starting current, bus voltage, starting torque, energy savings, slip, acceleration torque, and kVAR. The result of this research is that the best starting method is the VFD method.

2. METHOD

This research analyzes the inrush current in several induction motor starting methods. This aims to help researchers understand how to solve existing problems according to the expected results and can be scientifically justified. Meanwhile, the data for conducting this research was obtained from PT. Indonesia Asahan Aluminum is located at the Siguragura hydroelectric power plant (PLTA) in Paritohan Village, Toba Samosir Regency, North Sumatra Province, Indonesia. Next, analyze the starting current [2], [21], [22], bus voltage [23], [24], starting torque [25], [26], slip [27], [28], acceleration torque [29], and kVAR [30], [31] from each DOL, VFD, soft starting, and auto transformer method, as described in Figure 1.

Generator data for the Siguragura PLTA at PT. Inalum is as shown in Table 1. Furthermore, Siguragura PLTA has five (5) types of transformers, namely main transformer (MTR), distribution transformer (DT), station transformer (ST), local transformer (LT), and housing transformer (HT), as seen in Tables 2 to 6 respectively. Only the LT and HT are used in the ETAP software in the induction motor starting simulation series. Meanwhile, Siguragura hydroelectric power plant's disconnecting switch (DS) or PMS

separator has specifications that can be seen in Table 7. Next, the 3-phase induction motor being simulated is the main water supply pump (MWSM), which is useful as a pump for pumping water from the draft tube and flowing it to the generator's cooling system. The following 3-phase induction motor nameplate can be seen in Table 8.

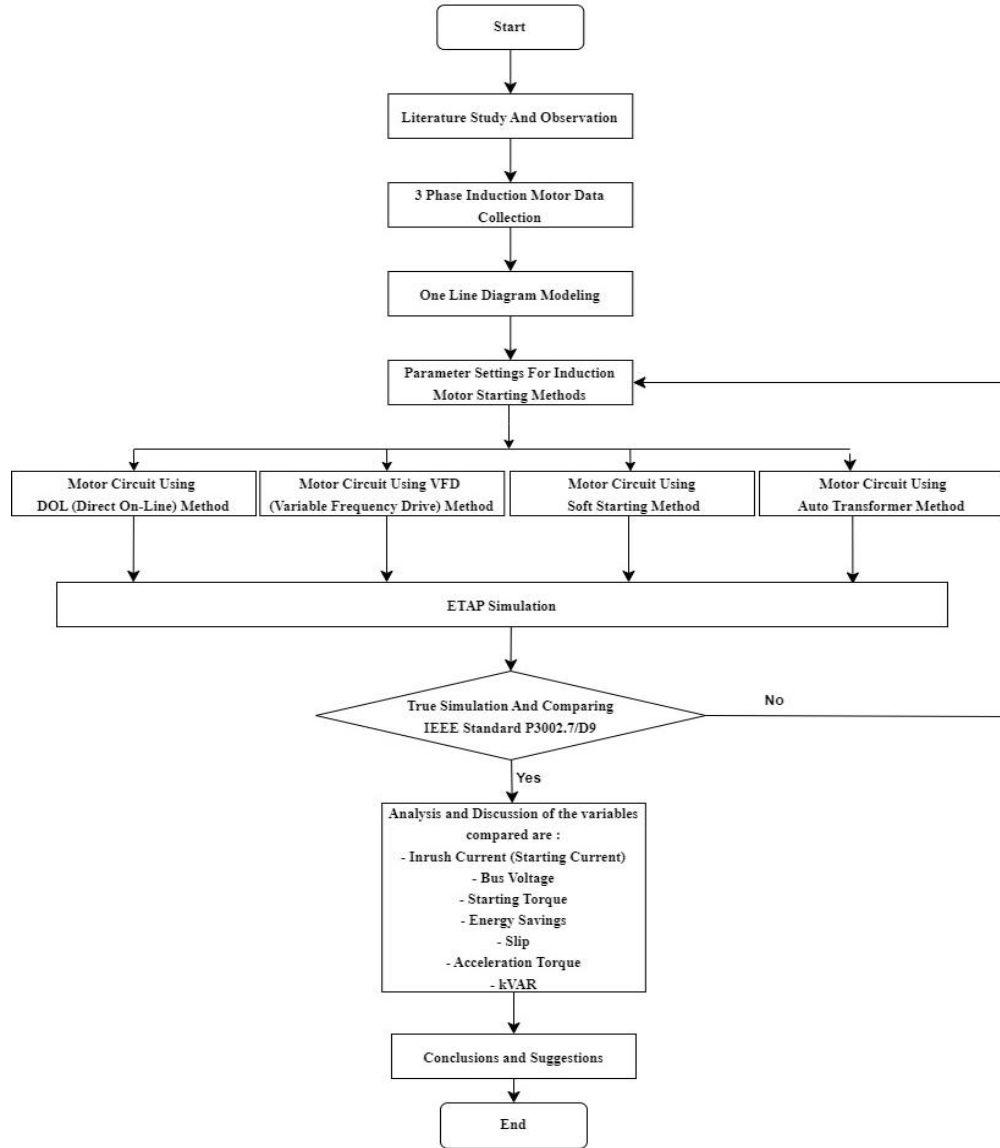


Figure 1. Research flow chart

Table 1. Generator data for the Siguragura hydroelectric power plant

Siguragura power station	
Output power	203 MW
Peak power	244 MW
Resistance per phase armature (75 C)	4.15 mΩ
Resistance per field phase (75 C)	0.16 Ω
Direct axis sinkron resistance (Xd)	97%
Direct axis transient resistance (Xd')	26%
Direct axis subtransient resistance (Xd'')	17%
Quadrature axis subtransient resistance (Xq'')	21%
Zero sequence resistance (X0)	7.50%
Negative sequence reactance (X2)	19%
Short circuit ratio	1.03
Apparent power	79.40 MVA

Table 2. MTR data for the Siguragura hydroelectric power plant

Main transformer	
Output power	79.4 MVA
Voltage	11 kV
Frequency	50 Hz
Power factor	0.90 lagging
HV value	281.25 kV
LV value	10.50 kV
HV tap parts	287.50 (F) – 281.25 (R) - 275 (F) kV
LV tap section	-
HV section	1050 kV
Neutral	200 kV
LV section	90 kV
Impedance voltage	14%
Manufacture	Toshiba corporation

Table 3. DT data for the Siguragura hydroelectric power plant

Distribution transformer	
Power capacity	3000 kVA
Frequency	50 Hz
Phase	3
Primary winding	6600 V
Secondary winding	22000 V
Impedance voltage	6.83%
Standard	JEC – 168 (1966)
Increase in oil temperature	50 °C
Cooling type	ONAN

Table 4. ST data for the Siguragura hydroelectric power plant

Station transformer	
Power capacity	300 kVA
Frequency	50 Hz
Phase	3
Primary winding	6600 V
Secondary winding	380 V
4.91 % impedance voltage	4.91%
Standard	JEC – 168 (1966)
Cooling type	ONAN
Increase in oil temperature	50 °C

Table 5. LT data for the Siguragura hydroelectric power plant

Local transformer	
Power capacity	1500 kVA
Frequency	50 Hz
Primary winding	10500 V
Secondary winding	6600 V
Impedance voltage	5.64%
Standard	IEC – 60076 – 11
ANAF	Cooling Type
Increase in oil temperature	120 °C

Table 6. HT data for the Siguragura hydroelectric power plant

Housing transformer	
Power capacity	500 kVA
Frequency	50 Hz
Primary winding	6600 V
Secondary winding	380 V
Impedance voltage	5.93%
Standard	JEC – 168 (1966)
Cooling type	AN
Increase in oil temperature	120 °C

Table 7. DS data for the Siguragura hydroelectric power plant

Disconnecting switch specifications	
Type and shape	Three phase, single throw, horizontal single breaker gang operated, rotating isolator, air type
Maximum voltage	300 kV, rms
Continuous current	1200 kA
Siguragura transmission and KTS transmission Transformer and bus tie	2000 kA
Second short time current	200 kA, 2 second
Control circuit voltage	100 VDC
Operating air pressure	15 kg/cm ²

Table 8. Three phase induction motor from the MWSP of the Siguragura hydroelectric power plant

Nameplate of the 3-phase induction motor	
Rated output	132 kW
Type	TIKK-FCKW11
Rated voltage	380 V
Rated current	236 A
Rated frequency	50 Hz
Rated speed	1485 rpm
Protection	IP54
Poles	4
Frame no.	280MD
Cooling method	IC411
Thermal class	F
Rating	CONT
Max. Amb	40 °C
Standard	JEC-2137-2000
Serial no.	E082J70HM
Manufactured	2008

Single line diagrams (SLD) are needed in this research to see the flow of electrical energy from the generator to the simulated 3-phase induction motor. The following SLD of Siguragura power station is seen in Figure 2. The SLD of Siguragura power station above has two (2) transmission lines, 20 DS, 75 buses, 50 circuit breakers (CB), 4 MTR (4), 3 DT, 2 ST, 2 LT, 5 HT, and four generators. In this SLD, the process of electrical energy flow from the generator to the 3-phase induction motor can be seen and simulated. Energy from the generator flows to the MTR and LT, from the LT the electrical energy is sent to the HT to reduce the voltage to 380 V, the electrical energy from the HT is used for distribution electricity to meet existing electricity needs at the underground Siguragura power station, MCC (motor control center) as well as existing synchronous generators. In this SLD, the 3-phase induction motor section that is simulated is in the common MCC section.

This research uses a one-line diagram design for starting a 3-phase induction motor to analyze all observed variables. In this design, there is one generator, 4 LT, 4 HT, 13 buses, 16 CB, 1 VFD, and four induction motors with the same specifications but different methods. To maximize simulation and analysis, each induction motor is given the same transformer specifications and cables to distribute the electric flow evenly. The following is the one-line diagram design for starting a 3-phase induction motor in Figure 3. In Figure 3, each induction motor has the same nameplate specifications but a different starting method. The description of each 3-phase induction motor can be seen in Table 9.

3. RESULTS AND DISCUSSION

3.1. Comparison of slips for each method

As shown in Figure 4, the VFD method experienced the most extreme and constant decrease in slip of the four other methods. The VFD method reaches a steady state quickly compared to other methods. The soft starting method decreases slip slowly; in other words, the soft starting method reduces slip more smoothly so that the motorbike does not experience shock. The following slip comparison graph data for each method can be seen in Table 10. DOL, the initial slip is 100% and is reduced slowly. The magnetic field speed (synchronous speed) initially has a very high value, while the rotor speed is initially stationary, so in the first second, the slip value is 100%. As time passes, the rotor moves to catch up with the magnetic field speed, so the slip value is 53 seconds (steady state condition), worth 0.995748%. VFD, seconds 0 to 1 slip has a value of 100% and drops drastically until the 11th-second steady-state conditions. The slip value is 0.030161%. According to the working principle of the VFD, the slip value drops so quickly and consistently that the motor speed can be constant. Soft starting, the initial slip is 100% and lowered slowly. As time

passes, the rotor moves to catch up with the speed of the magnetic field so that it reaches a steady state at the 58th second, which has a slip value of 0.995738%. Auto transformer, the initial slip is 100% and lowered slowly. As time passes, the rotor moves to catch up with the speed of the magnetic field until it reaches a steady state at the 54th second, which has a slip value of 0.995738%. The research results from slips for all methods are following previous research [16], [17].

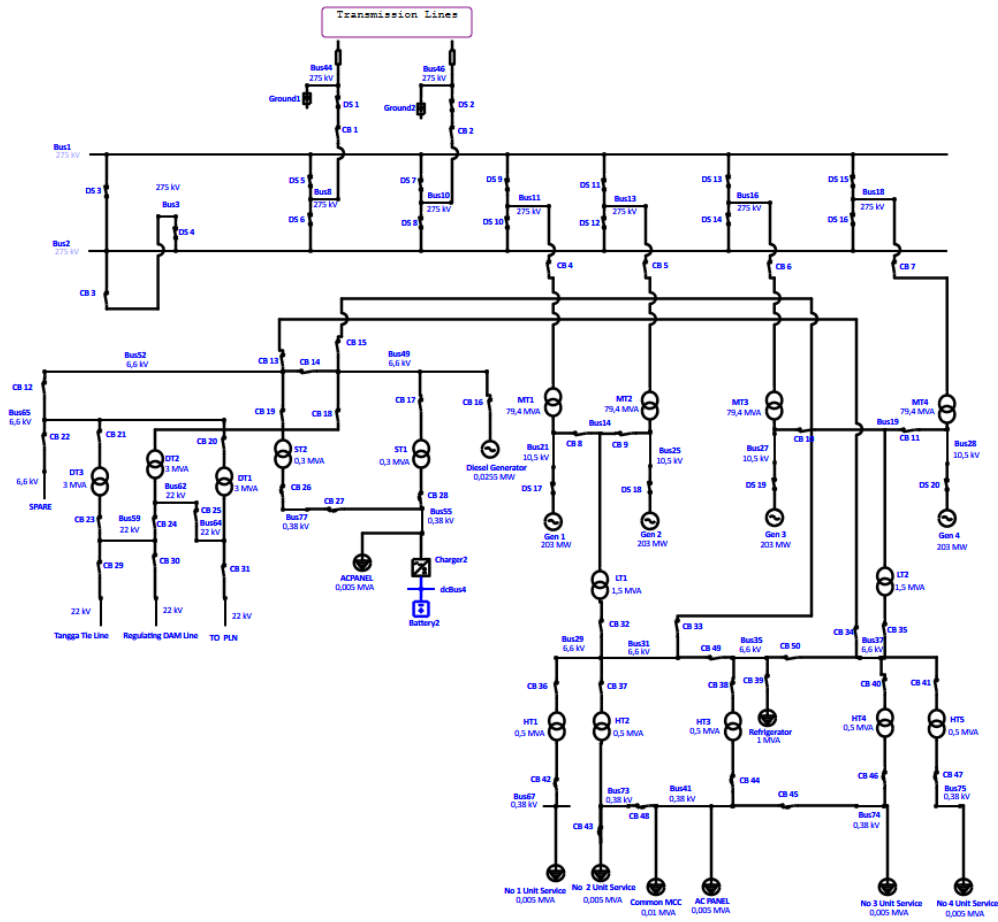


Figure 2. SLD of Sigurapura power station

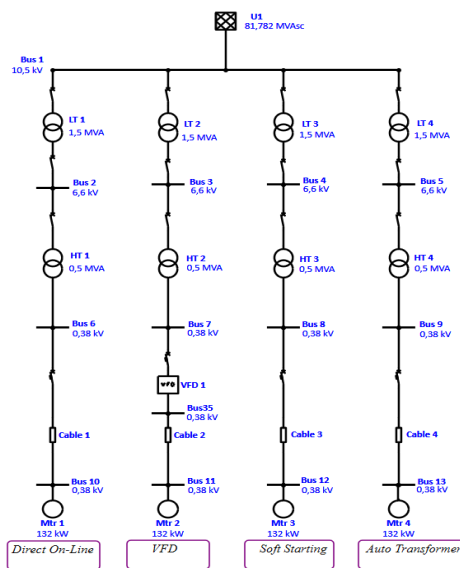


Figure 3. One line diagram design for starting a 3-phase induction motor

Design of starting a three phase induction motor using direct on-line ... (Yulianta Siregar)

Table 9. Description of each 3-phase induction motor in the circuit

Motor name	Starting method
DOL	Motor 1
VFD	Motor 2
Soft starting	Motor 3
Auto transformer	Motor 4

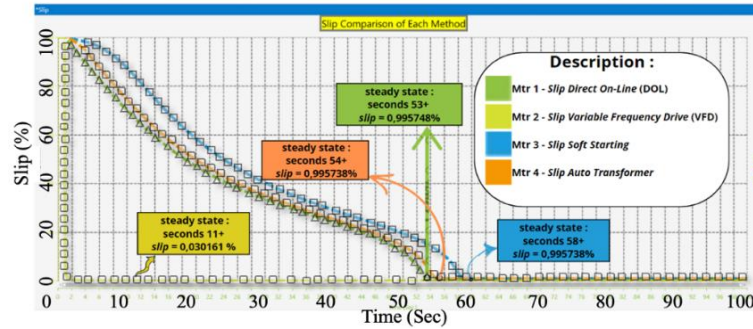


Figure 4. Slip for each method

Table 10. Results from comparison of slips for each method

Time interval (seconds)	Slip (%)			
	DOL	VFD	Soft starting	Auto transformer
0	100	100	100	100
20	46	0.03	57.93	48.66
40	21.70	0.03	27.63	23.21
60	0.99	0.03	0.99	0.99
80	0.99	0.03	0.99	0.99
100	0.99	0.03	0.99	0.99

3.2. Comparison of starting current for each method

As can be seen in Figure 5, the largest starting current is experienced by the DOL method, namely >500% full load amps (FLA), and the smallest starting current is experienced by the VFD method, namely <20% FLA. In the soft starting method, the starting current in the 1st second is 300% of the FLA and is increased gradually. In the auto transformer method, the starting current in the 1st second is 157.76% of the FLA; in the next second, it increases slowly. For a solution to overcome large starting currents, the DOL method is not suitable. The solution to this problem is to use the VFD method. The following graph data compares each method's starting/starting current, as seen in Table 11.

Starting current in DOL, the current spike in the DOL method is very large in the 1st second, reaching 563% of the nominal current. This can cause the motor to overheat, leading to potential damage and the cable to burn due to damage to the coil insulation. The prolonged high starting current in the DOL method, dropping to 350% of the nominal current only at the 45th second, underscores the need for caution. In the DOL method, the motor is steady from the 53rd second + at 94.12% of its nominal current. Meanwhile, in the VFD method, the surge current in the VFD method in the 1st second is still 0% of the FLA; in the 2nd second, the starting current is 19.83%. The largest starting current is at the 11th second, worth 252.2% of the nominal current. With its significantly lower starting current compared to the DOL method, the VFD method is a reassuring choice for managing high starting currents. In the VFD method, the motor reaches a steady state from the 11th second + at 86.5% of its nominal current. Furthermore, in the soft starting method, a current surge occurs in the 1st second, 300% of the FLA; in the 5th second, the starting current increases to 350%. The starting current in this method increases slowly. The largest starting current is in the 12th second, 502.5% of the nominal current. The starting current is better than the DOL method for the soft starting method but not better than the VFD method. In the soft starting method, the motor is steady from the 59th second + at 94.12% of its nominal current. Meanwhile, the autotransformer method experienced a current spike in the autotransformer method in the 1st second, amounting to 157.76% of the FLA; in the 4th second, the starting current increased to 545.26% of the FLA. The largest starting current is in the 4th second, 545.26% of the nominal current. The starting current is better than the DOL method for the autotransformer method but not better than the VFD and soft starting methods. In the auto transformer method, the motor reaches a steady state from the 55th second + at 94.12% of its nominal current.

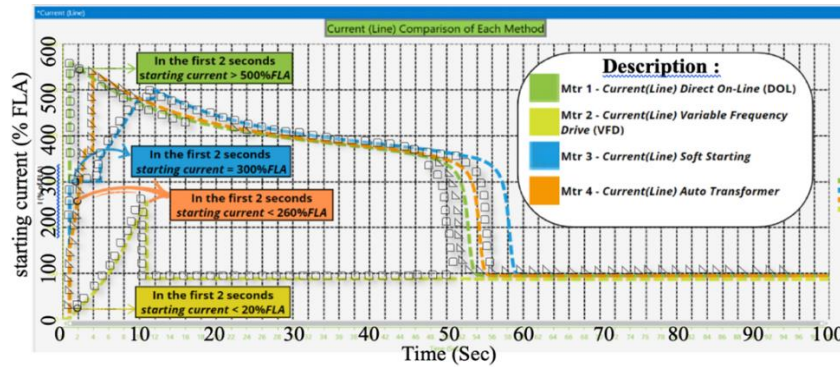


Figure 5. Motor starting current for each method

Table 11. Comparison results of starting current for each method

Time interval (seconds)	Current line (% FLA)			
	DOL	VFD	Soft starting	Auto transformer
1	563	0	300	157.76
2	551.50	19.83	300	257.63
3	540.38	36.22	300	372.95
4	529.38	53.81	300	545.26
5	519.02	73.57	350	534.22
6	509.18	96.12	375	523.64
7	499.90	121.83	400	513.56
8	491.17	150.74	425	504.01
9	482.99	182.56	450	495.03
10	475.37	216.70	480	486.61

3.3. Comparison of bus voltage for each method

As can be seen in Figure 6, at the 0th second, the bus voltage given to each method is 100%. In the 1st second, the largest bus voltage drop was experienced by the DOL method, namely 14.29%, and the smallest bus voltage drop by the VFD method was 0%. From the 0th to the 100th second, the highest bus voltage drop was experienced by the DOL method at 14.29%, so the bus voltage value was 85.71% of the nominal bus voltage at the 1st+ second, the lowest bus voltage drop was experienced by the VFD is 4.4% so that the bus voltage value is 95.6% of the nominal bus voltage at the 10th+ second. For a solution to overcome large bus voltage drops, the DOL method is not suitable. The solution to this problem is to use the VFD method. The following graph data compares the bus voltage for each method, as seen in Table 12.

In the DOL method, at the 0th second, the bus voltage is given at 100% of the nominal bus voltage; at the 1st second, the bus voltage drops to 85.71%, which has a difference of 14.29%. After that, the bus voltage continues to increase until it reaches a steady state at the 53rd second, which has a value of 97.4943924% of the nominal bus voltage. If this is separated from the 0th second, which is 100%, then the steady state voltage decreases by 2.5%. Next, in the VFD method, at the 0th second, the bus voltage is given at 100% of the nominal bus voltage. At the 1st second, the bus voltage is constant; at the 10th second, the bus voltage has decreased by 2.08%, so the value becomes 97.92% of the nominal bus voltage. After that, the bus voltage continues to increase until it reaches a steady state at the 11th second, with a value of 99.18479156% of the nominal bus voltage. If this is compared with the 0th second, which is 100%, then the steady state has a voltage drop of 0.8152%. From this, the VFD method effectively and efficiently overcame excessive bus voltage drops. Then, with the soft starting method, at the 0th second, the bus voltage is given at 100% of the nominal bus voltage; at the 1st second, the bus voltage drops by 6.98% so that the value becomes 93.01675415% of the nominal bus voltage, the biggest bus voltage drop in the 12th second it is 12.7%. Hence, the value is 87.3% of the nominal bus voltage. After that, the bus voltage continues to increase until it reaches steady at the 59th second, with a value of 97.4948349% of the nominal bus voltage. If you divide it with the 0th second, 100%, the steady state voltage decreases by 2.5%. Meanwhile, in the autotrformer method, in the 0th second, the bus voltage is given at 100% of the nominal bus voltage. In the 1st second, the bus voltage drops by 3.943%, so the value becomes 96.057% of the nominal bus voltage. The biggest decrease in bus voltage is in the 2nd second. 4 is 13.2% so the value is 86.2% of the nominal bus voltage. After that, the bus voltage continues to increase until it reaches a steady state at the 54th second, with a value of 97.4948349% of the nominal bus voltage. If you divide it with the 0th second, 100%, the steady state voltage decreases by 2.5%.

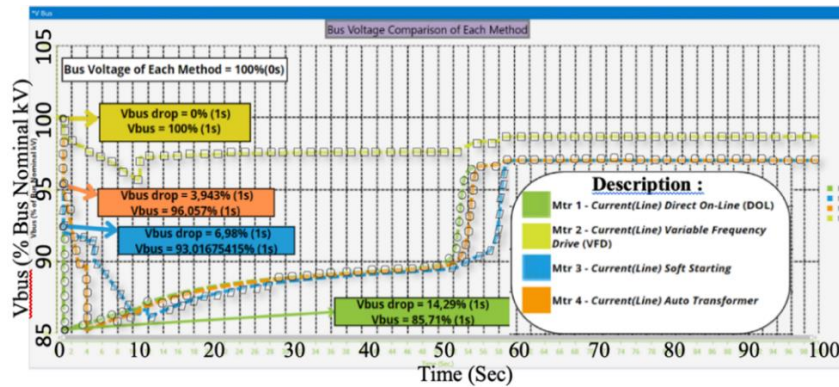


Figure 6. Bus voltage for each method

Table 12. Comparison results of bus voltage for each method

Time interval (seconds)	Bus voltage (% bus nominal kV)			
	DOL	VFD	Soft starting	Auto transformer
0	100	100	100	100
1	85.71	100	93.01	96.05
10	88.11	97.92	88.07	87.82
20	89.42	99.18	88.80	89.29
40	90.40	99.18	90.19	90.35
50	96.50	99.18	90.58	91.42
53	97.49	99.18	90.87	97.49
60	97.49	99.18	97.49	97.49
80	97.49	99.18	97.49	97.49
100	97.49	99.18	97.49	97.49

3.4. Comparison of acceleration torque for each method

As shown in Figure 7, the VFD method experiences the highest peak acceleration torque up to 282.083%. The method experiences the fastest acceleration torque in steady state conditions, namely at the 11th second, meaning that at the 11th second, the motor has reached its target speed, so the acceleration torque becomes 0%. The soft starting method is the method that takes the longest to reach a steady state, namely at 59 seconds, followed by the autotransformer method at 55 seconds and the DOL method at 54 seconds. Soft starting increases the acceleration torque slowly so the engine does not experience a large spike in acceleration torque in the first few seconds. The following graph data compares acceleration torque from each method, which can be seen in Table 13.

DOL method at 0 seconds, the motorbike is still stationary; at 1 second, the acceleration torque increases to 63.09%, meaning the motorbike is accelerating to reach its target speed. In the 10th second, the acceleration torque drops to 54.327%. The highest acceleration torque was obtained in the 49th second+ at 84.4%. At the 54th second, the acceleration torque has reached a steady state whose value is 0.000001807%; at this second, the motorbike has reached its target speed so that the acceleration torque is no longer needed. Then, for the VFD method, at 0 seconds, the motor is still stationary; at 1 second, the acceleration torque drops so that the value is -10%, meaning the motor is decelerating. In the 10th second, the acceleration torque increases so that the value becomes 180.945%; in this situation, the motorbike experiences large acceleration and rotation to reach its target speed. The highest acceleration torque is obtained in the 1st second+ at 285.5%. In the 11th second, the acceleration torque has reached a steady state whose value is 0%; at this second, it means the motor has reached its target speed, so the acceleration torque is no longer needed.

Furthermore, in the soft starting method, at 0 seconds, the motor is still stationary; at 1 second, the acceleration torque increases so that the value is 10.75%. In the 10th second, the acceleration torque increases, and the value becomes 53.09%. The motorbike experiences large acceleration and rotation to reach its target speed in this situation. The highest acceleration torque was obtained in the 55th second at 84.5%. In the 59th second, the acceleration torque has reached a steady state whose value is 0.00000018%; at this second, it means the motorbike has reached its target speed, so the acceleration torque is no longer needed. Meanwhile, for the autotransformer method, at 0 seconds, the motor is still stationary; at 1 second, the acceleration torque increases so that the value is 12.95%. In the 10th second, the acceleration torque increases to 57.648%. The motorbike experiences large acceleration and rotation to reach its target speed in this situation. The highest acceleration torque was obtained in the 51st second at 84.5%. At the 55th second, the acceleration torque has

reached a steady state, the value of which is 0.00000018%; at this second, the motorbike has reached its target speed, so the acceleration torque is no longer needed.

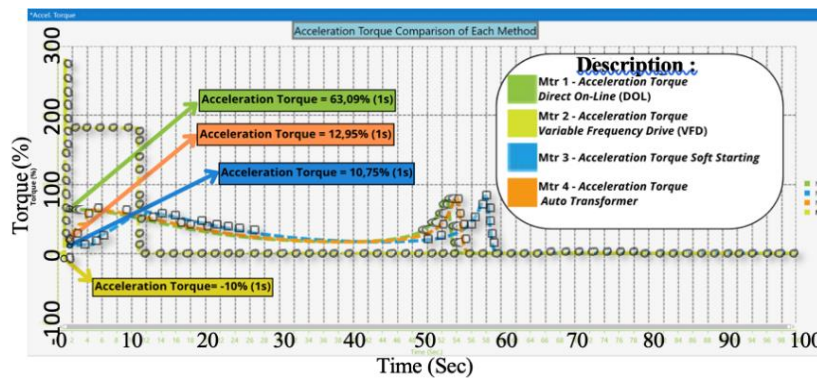


Figure 7. Acceleration torque for each method

Table 13. Comparison results of acceleration torque for each method

Time interval (seconds)	Acceleration torque (% torque)			
	DOL	VFD	Soft starting	Auto transformer
1	63.09	-10	10,75	12.95
10	54.32	180.94	53.09	57.64
20	31.78	31.77	43.87	34.44
30	20.32	0	25.50	21.30
40	19.72	0	18.62	18.95
50	30.44	0	26.23	67.54
60	0	0	0	0

3.4. Comparison of motor torque for each method

As seen in Figure 8, the VFD method has the highest motor starting torque, reaching 291.5% in the 1st+ second, and the soft starting method has the lowest starting torque of 20.75%. The soft starting method is the method that takes the longest to reach a steady state, namely at 59 seconds, followed by the autotransformer method at 55 seconds and the DOL method at 53 seconds. The VFD method is the fastest to reach a steady state in the 11th+ second. The highest peak motor torque was experienced by the VFD method at 291.5%. The following graph data compares motor torque from each method, as seen in Table 14.

In the DOL method, the motor is stationary at 0 seconds. At 1 second, the motor torque increases to 73.09%. In the 10th second, the motor torque decreases, so the value becomes 62.3%. The highest motor torque is obtained in the 49th second+, at 173%. At 53+ seconds, the motor torque has reached a steady state of 91.89%. Then, for the VFD, at 0 seconds, the motor is still at rest. In the 1st second, the motor torque remains at 0% but immediately increases drastically at 1.1 seconds to 291.5%. In the 10th second, the motor torque increases drastically, so the value becomes 261.75%. The highest motor torque was obtained in the 11th second at 273%, but this spike in motor torque did not last long because, at 11+ seconds, the motor torque reached a steady state of 92.97%. Compared with the DOL method, the VFD method reaches steady state conditions more quickly, and the motor torque at steady state conditions is greater than that of the DOL method. Further, in the soft starting method, at 0 seconds, the motor is still stationary; at 1 second, the motor torque increases to 20.75%. In the 10th second, the motor torque increased to 56.45%. The increase in motor torque is done slowly (not increasing drastically or decreasing drastically). The highest motor torque was obtained in the 55th second at 172.9%. The motor torque is steady at the 59th+ second, worth 91.89%. Compared with the DOL method, the soft starting method has a smaller motor starting torque in the 1st second and reaches a steady state longer than the DOL method. Meanwhile, with the autotransformer method, at 0 seconds, the motor is still stationary; at 1 second, the motor torque increases to 22.95%. In the 10th second, the motor torque increased to 63.14%. The highest motor torque is obtained in the 50th second+ at 172.9%. The motor torque is steady at the 55th+ second, worth 91.89%. Compared with the DOL method, the autotransformer method has a smaller motor starting torque in the 1st second and reaches a steady state longer than the DOL method but faster than the soft starting method.

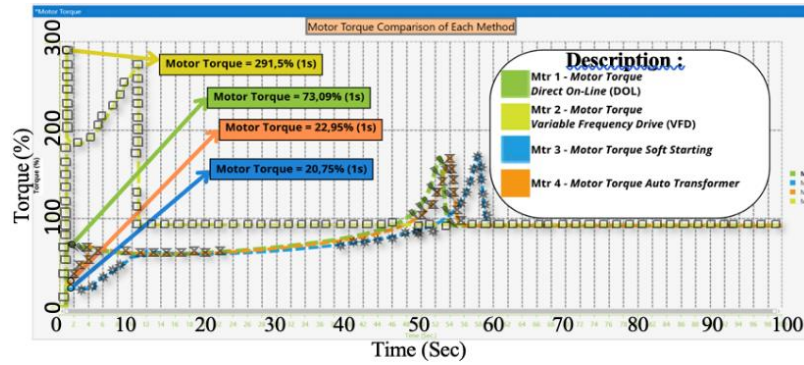


Figure 8. Motor torque for each method

Table 14. Comparison results of motor torque for each method

Time interval (seconds)	4 motor torque (% torsi)			
	DOL	VFD	Soft starting	Auto transformer
1	73.09	291.50	20.75	22.95
10	62.30	261.75	56.45	63.14
20	63.06	92.97	61.45	62.43
30	70.41	92.97	65.60	69.05
40	84.74	92.97	75.17	81.80
50	121.80	92.97	98.55	152.20
60	91.89	92.97	91.89	91.89

3.5. Comparison of electrical kW for each method

As seen in Figure 9, the highest peak electrical kW was owned by the VFD method, reaching 368.7 kW, but the use of electrical kW stabilized the fastest at the 11th+ second, while the other methods reached a stable state at the 50th+ second. The method with the largest kW electrical usage is the DOL method, which is energy-intensive compared to other methods. The following graphical data compares kW electrical for each method, as described in Table 15. Table 15 shows the difference in total energy use for each method. Data on the amount of kW electricity from each method was taken at the 1st second, 10th second, 20th second, 30th second, 40th second, 50th second, and 60th second. The case in this research uses the DOL method, which uses 1,034 kW of energy. If you use the VFD method of 965.73 kW, the energy savings will be 68.27 kW. If you use the soft starting method, 885.98 kW, the energy savings will be 148.02 kW. If you use the autotransformer method, which is 970.50 kW, the energy savings will be 63.5 kW. The most energy-efficient method is soft starting.

In the DOL method, the motor's active power is 182 kW in the first second and decreases to 143 kW in the 10th second. The highest energy in the DOL method occurs at the 49th+ second, 247.7 kW. The stable energy is 125 kW from the 51st second. If data is taken from the 1st second, 10th second, 20th second, 30th second, 40th second, 50th second, and 60th second, the total energy used is 1,034 kW. Meanwhile, in the VFD method, in the 1st second, the motor has an active power of 1 kW, which increases drastically in the 10th second to 319,728 kW. The highest energy in the VFD method occurred in the 11th second at 368.7 kW. Stable energy of 129 kW from the 11th second+. If data is taken from the 1st second, 10th second, 20th second, 30th second, 40th second, 50th second, and 60th second, the total energy used is 965.73 kW. Then, the soft starting method occurs in the first second. The motor has an active power of 51.58 kW and increases in the 10th second to 136.49 kW. The highest energy in the soft starting method occurs at the 55th second, 247 kW. Stable energy of 125 kW from the 59th second+. If data is taken from the 1st second, 10th second, 20th second, 30th second, 40th second, 50th second, and 60th second, the total energy used is 885.98 kW. Furthermore, in the 1st second of the motor, the autotransformer method has an active power of 57.06 kW and increases in the 10th second to 147.123 kW. The highest energy in the autotransformer method occurs in the 50th second + at 247 kW. Stable energy of 125 kW from the 55th second+. If data is taken from the 1st second, 10th second, 20th second, 30th second, 40th second, 50th second, and 60th second, the total energy used is 970.50 kW.

3.6. Comparison of kVAR for each method

As shown in Figure 10, 1st second, the highest kVAR value is owned by the DOL method, and the lowest kVAR value is owned by the VFD method. The highest peak kVAR value is the DOL method of 695.8 kVAR, then the auto transformer method of 670.84 kVAR, then the soft starting method of 629 kVAR,

and the smallest method is the VFD of 0 kVAR. A high kVAR can cause low power factor and poor power quality and can even cause excessive electricity bills. The best method to overcome kVAR is VFD because the efficiency is 100%, and in the VFD, there is a capacitive load that can balance the inductive load that uses kVAR. The following kVAR comparison graph data for each method can be seen in Table 16.

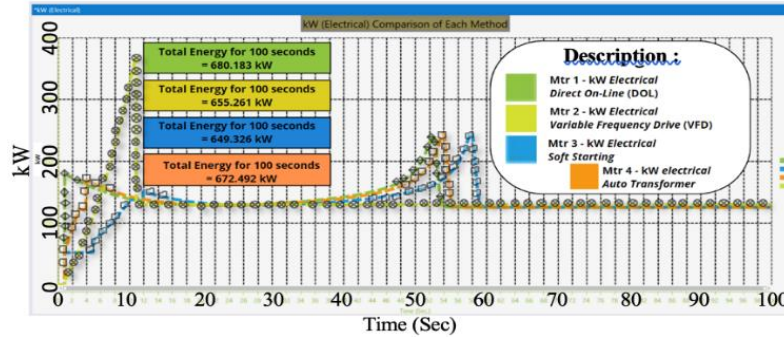


Figure 9. Electrical kW for each method

Table 15. Comparison results of electrical kW for each method

Time interval (seconds)	kW electrical (kW)			
	DOL	VFD	Soft starting	Auto transformer
1	182	1	51.58	57.06
10	143	319.72	136.49	147.12
20	132	129	135.41	132.08
30	135	129	132	134.31
40	150	129	139.80	146.74
50	167	129	165.70	228.18
60	125	129	125	125
Total kW	1034	965.73	885.98	970.50

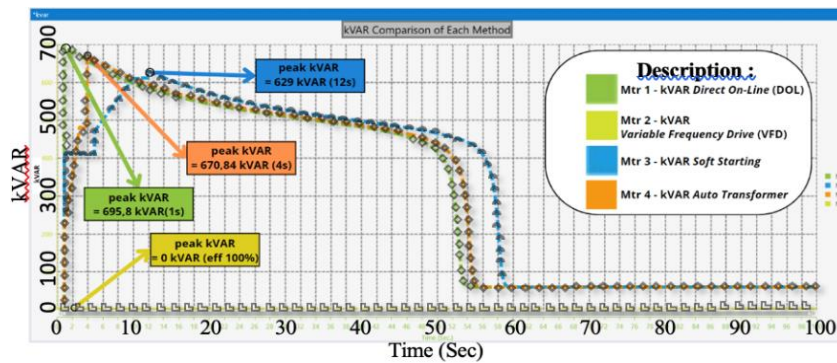


Figure 10. kVAR for each method

Table 16. Comparison results of kVAR for each method

Time interval (seconds)	kVAR			
	DOL	VFD	Soft starting	Auto transformer
1	695.8	0	41.3	221.1
10	614.815	0	622.25	626.88
20	554.67	0	584.67	561.24
30	518.49	0	537.61	523
40	484.77	0	505.14	490.46
50	86.6462	0	460.5	355.28
60	58.96	0	58.9	58.9

In the DOL method, the motor's reactive power is 695.8 kVAR in the first second and decreases to 614.815 kVAR in the 10th second. The kVAR value in the first second experienced a very large spike; the greater the kVAR value, the smaller the power factor. The highest kVAR in the DOL method occurs in the

first second at 704.19 kVAR, which decreases as time increases. The motor has a stable energy of 58.96 kVAR for 53+ seconds. Meanwhile, the VFD method does not have kVAR, so the power quality/power factor is good because the efficiency is 100%. This can save electricity bills and maximize apparent power usage without power loss. Then, the soft starting method in the 1st second of the motor has a reactive power of 417.3 kVAR and increases in the 10th second to 622.25 kVAR. The kVAR value in the 1st second experienced a big spike, but not as big as the DOL method. The highest kVAR in the soft starting method occurs in the 12th+ second at 629 kVAR and decreases as time increases. Stable energy of 58.9 kVAR from 59+ seconds. The soft starting method has a lower kVAR spike than the DOL method, which is 695.8 kVAR. Next is the autotransformer method; in the 1st second, the motor has a reactive power of 221.1 kVAR and increases in the 10th second to 626.88 kVAR. The kVAR value in the 1st second experienced a spike, but not as big as the DOL and soft starting methods. The highest kVAR in the autotransformer method occurs in the 4th+ second at 670.84 kVAR and decreases as time increases. Stable energy of 58.9 kVAR from the 55th second+. The autotransformer method has a lower peak kVAR value than the DOL method, which is 695.8 kVAR, and higher than the soft starting method, which is 629 kVAR.

4. CONCLUSION

This research evaluated four methods: the direct-on-line method, variable-frequency drive, soft starting, and autotransformer. Among these, the VFD method emerged as the most efficient, reaching a steady slip state at the fastest pace. In contrast, the soft starting method, while taking the longest to reach steady state slip, proved to be the most energy efficient. The DOL method, on the other hand, exhibited the largest starting current, which lasted a significant duration. Even in this aspect, the VFD method outperformed, showcasing the smallest starting current. Then, the DOL method experienced the highest decrease in bus voltage, and the VFD method experienced the lowest decrease. A decrease in bus voltage can damage the performance of electrical equipment because it does not operate according to its nominal voltage. The greater the bus voltage drop, the worse the electrical power system. Meanwhile, the acceleration torque of the VFD method reaches a steady state faster than other methods, meaning that the VFD method quickly reaches its target speed. Meanwhile, the soft starting method takes the longest to reach the acceleration torque steady state because the soft starting operator gradually/slowly decreases or increases the acceleration. Furthermore, the VFD method has the largest starting torque, and the soft starting method has the smallest. The VFD has the largest starting torque because at the 11th second, it has reached a steady state, so the starting torque is large so that it can operate optimally, while the soft starting method has a small starting torque because the operation of this method is carried out in stages. Moreover, if we consider the active power (kW) data at various time intervals from each method, we find that the DOL method consumes the highest at 1,034 kW, while the soft starting method is the most energy efficient, consuming the lowest at 885.98 kW. This underscores the cost-effectiveness of the soft starting method, making it a compelling choice for energy-conscious applications. Further, the DOL method owns the highest kVAR value. The VFD method owns the lowest kVAR value because the VFD used is 100% efficient. The greater the kVAR value, the lower the power factor, resulting in poor power quality because a lot of power is wasted. So, the suitable method to overcome this is VFD. The final conclusion is that the best induction motor starting method in this research is the VFD method, and the soft starting method offers the best energy savings.

ACKNOWLEDGEMENTS

The authors thank the Ministry of Higher Education Malaysia for funding this study. This work was supported by the Indonesian Collaboration Research in 2024




REFERENCES

- [1] M. Soleimani, M. N. Alizadeh, and M. Moallem, "Economical replacement decision for induction motors in industry," in *2018 IEEE Texas Power and Energy Conference (TPEC)*, Feb. 2018, pp. 1–6, doi: 10.1109/TPEC.2018.8312086.
- [2] M. Habyarimana and D. G. Dorrell, "Methods to reduce the starting current of an induction motor," in *2017 IEEE International Conference on Power, Control, Signals and Instrumentation Engineering (ICPCSI)*, Sep. 2017, pp. 34–38, doi: 10.1109/ICPCSI.2017.8392319.
- [3] C. Yang *et al.*, "Starting current analysis in medium voltage induction motors: detecting rotor faults and reactor starting defects," *IEEE Industry Applications Magazine*, vol. 25, no. 6, pp. 69–79, Nov. 2019, doi: 10.1109/MIAS.2019.2923105.
- [4] M. Akbaba, "A novel simple method for elimination of DOL starting transient torque pulsations of three-phase induction motors," *Engineering Science and Technology, an International Journal*, vol. 24, no. 1, pp. 145–157, Feb. 2021, doi: 10.1016/j.jestch.2020.06.007.
- [5] I. N. Sukarma, I. K. Ta, and I. M. Sajayasa, "Comparison of three phase induction motor start using DOL, Star Delta and VSD Altivar61," *Journal of Physics: Conference Series*, vol. 1450, no. 1, p. 012045, Feb. 2020, doi: 10.1088/1742-6596/1450/1/012045.




- [6] L. Hardine, D. B. Santoso, and R. S. Hadikusuma, "Analysis of the influence of star delta system in reduce electric starting surge in 3 phase motors," *Electrician*, vol. 16, no. 2, pp. 208–214, May 2022, doi: 10.23960/elc.v16n2.2288.
- [7] S. N. S. Hubais, C. B. Moorthy, J. Santiago, S. S. S. Masan, and Y. S. Al Din Arfah, "IoT star-delta starter for remote control of 3-phase motors," in *2022 IEEE 5th Student Conference on Electric Machines and Systems (SCEMS)*, Nov. 2022, pp. 1–5, doi: 10.1109/SCEMS56272.2022.9990667.
- [8] F. Chiranga and L. Masisi, "Managing inrush current in a variable speed drive short term power interruption ride-through module," in *IECON 2021 – 47th Annual Conference of the IEEE Industrial Electronics Society*, Oct. 2021, pp. 1–6, doi: 10.1109/IECON48115.2021.9589119.
- [9] S. Serhiienco and O. Khrebtova, "Starting torque of variable frequency electric drive," in *2017 International Conference on Modern Electrical and Energy Systems (MEES)*, Nov. 2017, pp. 104–107, doi: 10.1109/MEES.2017.8248862.
- [10] T. H. Blair, "Variable frequency drive systems," in *Energy Production Systems Engineering*, Wiley, 2016, pp. 441–466.
- [11] Y. Sapkota, S. Devkota, V. Borra, P. Cortes, S. Itapu, and F. Li, "Harmonic content analysis of a soft starting variable frequency motor drive based on FPGA," in *2023 IEEE 3rd International Conference on Sustainable Energy and Future Electric Transportation (SEFET)*, Aug. 2023, pp. 1–5, doi: 10.1109/SeFeT57834.2023.10245108.
- [12] V. Tytiuk, Z. Rozhnenko, M. Baranovska, A. Berdai, O. Chorny, and V. Saravas, "Soft starters of powerful electric motors and economic aspects of their application," in *2020 IEEE Problems of Automated Electrodrive. Theory and Practice (PAEP)*, Sep. 2020, pp. 1–4, doi: 10.1109/PAEP49887.2020.9240859.
- [13] F. Jiang, C. Tu, Q. Guo, Z. Wu, and Y. Li, "Adaptive soft starter for a three-phase induction-motor driving device using a multifunctional series compensator," *IET Electric Power Applications*, vol. 13, no. 7, pp. 977–983, Jul. 2019, doi: 10.1049/iet-epa.2018.5079.
- [14] J. Yuan, C. Wang, S. Yin, L. Wei, K. Muramatsu, and B. Chen, "Coupled autotransformer and magnetic-control soft-start method for super-large-capacity high-voltage motors," *High Voltage*, vol. 5, no. 1, pp. 38–45, Feb. 2020, doi: 10.1049/hve.2019.0007.
- [15] D. Penkov and C. Gaudeaux, "MV motors starting with auto-transformer," in *2018 Petroleum and Chemical Industry Conference Europe (PCIC Europe)*, Jun. 2018, pp. 1–9, doi: 10.23919/PCICEurope.2018.8491415.
- [16] A. Zaw Latt, "Three phase induction motor starting analysis using ETAP," *International Journal of Latest Technology in Engineering*, vol. VIII, no. IV, pp. 145–149, 2019.
- [17] O. Osita, P. I. Obi, and I. K. Onwuka, "Induction motor starting analysis and start aided device comparison using ETAP," *European Journal of Engineering Research and Science*, vol. 2, no. 7, p. 1, Jul. 2017, doi: 10.24018/ejers.2017.2.7.348.
- [18] S. M. Al-Refai, "Starting analysis of three-phase squirrel cage induction motors. case study: oil production field in Libya," in *2023 IEEE 3rd International Maghreb Meeting of the Conference on Sciences and Techniques of Automatic Control and Computer Engineering (MI-STA)*, May 2023, pp. 117–123, doi: 10.1109/MI-STA57575.2023.10169599.
- [19] X. Liang and O. Ilochonwu, "Induction motor starting in practical industrial applications," *IEEE Transactions on Industry Applications*, vol. 47, no. 1, pp. 271–280, Jan. 2011, doi: 10.1109/TIA.2010.2090848.
- [20] R. L. Chakrasali, V. R. Sheelavant, and H. N. Nagaraja, "A novel method of starting induction motor - a comparative study," *International Journal of Power Electronics and Drive Systems (IJPEDS)*, vol. 1, no. 1, pp. 41–46, Sep. 2011, doi: 10.11591/ijpeds.v1i1.70.
- [21] M. Habyarimana, D. G. Dorrell, and R. Musumpuka, "Reduction of starting current in large induction motors," *Energies*, vol. 15, no. 10, p. 3848, May 2022, doi: 10.3390/en15103848.
- [22] Ermawati, F. Palaha, Yolnasdi, E. H. Arya, Machdalena, and E. Yusrinal, "Analysis of starting current and electrical energy in three phase induction motor as a chemical processing system in PT Riau Andalan Pulp & Paper," in *2022 9th International Conference on Electrical Engineering, Computer Science and Informatics (EECSI)*, Oct. 2022, pp. 264–269, doi: 10.23919/EECSI56542.2022.9946635.
- [23] A. Hota and V. Agaral, "A Novel Three-Phase induction motor drive with voltage boosting capability, low current THD and low common mode voltage," in *2020 IEEE International Conference on Power Electronics, Drives and Energy Systems (PEDES)*, Dec. 2020, pp. 1–4, doi: 10.1109/PEDES49360.2020.9379655.
- [24] L. Gumilar, A. N. Afandi, Sujito, and M. R. Faiz, "Starting induction motor at different voltage levels in the electrical power system," in *2021 International Conference on Electrical and Information Technology (IEIT)*, Sep. 2021, pp. 269–273, doi: 10.1109/IEIT53149.2021.9587354.
- [25] M. A. A. Ismail, J. Windelberg, and G. Liu, "Simplified sensorless torque estimation method for harmonic drive based electro-mechanical actuator," *IEEE Robotics and Automation Letters*, vol. 6, no. 2, pp. 835–840, Apr. 2021, doi: 10.1109/LRA.2021.3052392.
- [26] P. Khaledian, B. K. Johnson, and S. Hemati, "Harmonic mitigation and a practical study of torque harmonics in induction motor startup," in *2018 IEEE Power & Energy Society General Meeting (PESGM)*, Aug. 2018, pp. 1–5, doi: 10.1109/PESGM.2018.8586670.
- [27] Y. Fu, L. Cheng, J. Yu, X. Duan, and H. Tian, "Sideband harmonics identification and application for slip estimation of induction motors based on a self-adaptive wiener filter," *IEEE Transactions on Instrumentation and Measurement*, vol. 72, pp. 1–12, 2023, doi: 10.1109/TIM.2023.3289561.
- [28] Y. Maouche, M. El Kamel Oumaamar, M. Boucherma, and A. Khezzar, "A new approach for broken bar fault detection in three-phase induction motor using instantaneous power monitoring under low slip range," *International Journal of Electrical and Computer Engineering (IJECE)*, vol. 4, no. 1, pp. 52–63, Feb. 2014, doi: 10.11591/ijece.v4i1.4611.
- [29] M. Toman, R. Cipin, M. Mach, and P. Vorel, "Application of acceleration method for evaluation of induction motor torque-speed characteristics," in *2017 IEEE International Conference on Environment and Electrical Engineering and 2017 IEEE Industrial and Commercial Power Systems Europe (EEEIC / I&CPS Europe)*, Jun. 2017, pp. 1–4, doi: 10.1109/EEEIC.2017.7977585.
- [30] B. Peng, L. Liu, and J. Wang, "Design of harmonic control and reactive power compensation scheme in a pipe fitting factory," in *2021 China International Conference on Electricity Distribution (CICED)*, Apr. 2021, pp. 107–110, doi: 10.1109/CICED50259.2021.9556833.
- [31] A. Michaelides and T. Nicolaou, "A variable inductor-capacitor for reactive power compensation," in *2023 13th International Symposium on Advanced Topics in Electrical Engineering (ATEE)*, Mar. 2023, pp. 1–6, doi: 10.1109/ATEE58038.2023.10108301.

BIOGRAPHIES OF AUTHORS






Yulianta Siregar    was born July 09, 1978 in Medan, North Sumatera Utara, Indonesia. He did his undergraduate work at University of Sumatera Utara in Medan, North Sumatera Utara, Indonesia. He received a Bachelor of Engineering in 2004. After a while, he worked for a private company. He continued taking a master's program in Electrical Engineering at the Institute of Sepuluh Nopember, Surabaya, West Java, Indonesia, from 2007-2009. He was in a Ph.D. program at Kanazawa University, Japan, from 2016-2019. Until now, he lectured at Universitas Sumatera Utara. He can be contacted at email: julianta_srg@usu.ac.id.






Yosephine Rotua Oktaviana Siahaan    is a fresh graduate of Electrical Engineering bachelor's degree from Universitas Sumatera Utara in 2024. Until now, she has been an Electrical Energy Conversion Laboratory assistant in the Electrical Engineering Department, Universitas Sumatera Utara. Her research area field study is an electrical power system. She can be contacted at email: yosephinesiahaan.ys@gmail.com.






Nur Nabila Binti Mohamed    was born on January 04, 1989 in Pahang, Malaysia. She obtained her Bachelor of Engineering from Shibaura Institute of Technology, Japan in year 2012. In 2015, she received Master of Science in Electrical Engineering and obtained Ph.D. in the same field in 2019 from Universiti Teknologi MARA, Selangor. She started her career as a lecturer and programme coordinator at the Department of Electrical and Electronics Engineering, Mahsa University, Selangor, Malaysia from January 2019 to June 2023. Currently, she is working as a senior lecturer at Universiti Teknologi MARA, Selangor, Malaysia. Her research interest is on internet of things, information security, network security, and security for lightweight protocol. She can be contacted at email: numabilamohamed@uitm.edu.my.



Dedet Candra Riawan    was born November 19, 1973 in Blitar, West Java, Indonesia. He did his undergraduate at Institut Teknologi Sepuluh Nopember in Surabaya, West Java, Indonesia. He received a Bachelor of Engineering in 1999. He continued taking a master's program in Electrical Engineering at the Curtin University, Perth, Australia, from 2005-2007. He was in a Ph.D. program at Curtin University, Perth, Australia, from 2007-2010. Until now, he lectured at Institut Teknologi Sepuluh Nopember. He can be contacted at email: dedet.riawan@its.ac.id.



Muldi Yuhendri    received bachelor degree in Electrical Engineering Education from Universitas Negeri Padang (UNP), Padang, Indonesia in 2005. He received M.T. and Dr. degrees in Electrical Engineering from Institut Teknologi Sepuluh Nopember (ITS), Surabaya, Indonesia in 2009 and 2017, respectively. He has joined Universitas Negeri Padang as a lecturer in the Electrical Engineering Department since 2006. He is the head of the industrial electrical engineering study program, Faculty of Engineering, Universitas Negeri Padang. He also served as chairman of instrument, control and automation research group, Universitas Negeri Padang. His research interests are power electronic, electric drive, electrical machines, power converter for renewable energy system, and intelligent control. He can be contacted at email: muldiy@ft.unp.ac.id.